

Full Length Article

Propionic acid induces mitochondrial dysfunction and affects gene expression for mitochondria biogenesis and neuronal differentiation in SH-SY5Y cell line



Soon Ae Kim^{a,*}, Eun Hye Jang^a, Mun Ji Young^b, Hyosun Choi^{b,c}

^a Department of Pharmacology, School of Medicine, Eulji University, Daejeon, Republic of Korea

^b Neural Circuits Research Group, Korea Brain Research Institute, Daegu, Republic of Korea

^c BK21 Plus Program, Department of Senior Healthcare, Graduate School, Eulji University, Daejeon, Republic of Korea

ARTICLE INFO

Keywords:

Propionic acid
Mitochondria
Notch signaling
Neuronal cells

ABSTRACT

Studies in animal models have shown that the short-chain fatty acid, propionic acid (PPA), interferes with mitochondrial metabolism leading to mitochondrial dysfunction and behavioral abnormalities. The aim of this study was to investigate the effects of PPA on mitochondrial function and gene expression in neuronal cells. SH-SY5Y cells and normal human neural progenitor (NHNP) cells were exposed to 1, 5 mM PPA for 4 or 24 h and we found that the mitochondrial potential measured in SH-SY5Y cells decreased in a dose-dependent manner after PPA treatment. Electron microscopy analysis revealed that the size of the mitochondria was significantly reduced following PPA treatment. A dose-dependent increase in the mitochondrial DNA copy number was observed in the PPA-treated cells. The expression of the mitochondrial biogenesis-related proteins PGC-1 α , TFAM, SIRT3, and COX4 was significantly increased after PPA treatment. Transcriptome analysis revealed that mRNA expression in the notch signaling-related genes *ASCL1* and *LFNG* changed after PPA treatment and the positive correlated protein expression changes were also observed. These results revealed that PPA treatment may affect neurodevelopment by altering mitochondrial function and notch signaling-related gene expression.

1. Introduction

Propionic acid (PPA) is an important intermediate of cellular mitochondrial metabolism and modulates fatty-acid metabolism, suppresses inflammation, and exerts antibacterial effects. PPA is found in foods and is produced by the microbiome; in contrast, 3-nitropropionic acid (3NP), a chemical derivative of PPA, is a potential food contaminant and a potent mitochondrial neurotoxin. PPA is also associated with mitochondrial dysfunction-related disorders, including propionic acidemia in humans (Frye et al., 2016). It is shown that oxidative stress markers (e.g., lipid peroxidation) are increased, coupled with a decrease in the activities of glutathione, glutathione peroxidase, and catalase in the biochemical analyses of brain homogenates from PPA-treated rats (El-Ansary et al., 2012). In addition, carnosine, carnitine, N-acetylcysteine, and vitamin D have been suggested as supplements to overcome PPA neurotoxicity (Aldbass et al., 2013; Alfawaz et al., 2014; El-Ansary et al., 2013). It is also suggested that PPA may have additional bioactive effects on intracellular acidification/calcium release,

gap junction gating, immune function, and the alteration of gene expression (MacFabe, 2013, 2012).

PPA has also been reported to induce neurotoxicity through the depletion of important neurotransmitters, such as GABA and serotonin, and to cause genotoxic effects, such as a highly significant increase in tail length, percentage of tail DNA damage, and tail moment (Al-Ghamdi et al., 2014). Moreover, it has been reported that PPA treatment alters phospholipid molecular species in the brain and plasma, including acylcarnitine, which allows the identification of biomarkers of abnormal mitochondrial fatty acid metabolism in animal models (MacFabe, 2012; Thomas et al., 2012). It has also been observed that up to 17% of children with autism spectrum disorders (ASD) manifest biomarkers of abnormal mitochondrial fatty-acid metabolism, which parallel biomarkers observed in the PPA-induced rodent model of ASD (Frye et al., 2013). In several studies, mitochondrial dysfunction and oxidative stress were suggested as possible pathogeneses, as per the evidence observed in several metabolic disorders with ASD phenotypes, such as phenylketonuria disorders of purine metabolism, cerebral folate

* Corresponding author at: Department of Pharmacology, School of Medicine, Eulji University, 77, Gyeryong-ro 771beon-gil, Jung-gu, Daejeon, 34824, Republic of Korea.

E-mail address: sakim@eulji.ac.kr (S.A. Kim).

<https://doi.org/10.1016/j.neuro.2019.09.009>

Received 13 May 2019; Received in revised form 27 August 2019; Accepted 12 September 2019

Available online 14 September 2019

0161-813X/ © 2019 Elsevier B.V. All rights reserved.

deficiency, and propionic acidemia (Al-Owain et al., 2013; Goldani et al., 2014; Yoo et al., 2017). Several behavioral animal studies of PPA treatment have found ASD-like behavior (Choi et al., 2018; Rouillet et al., 2013; Shultz et al., 2008). PPA is a type of short chain fatty acid that has histone deacetylase inhibitory effects, like those of valproic acid, which is commonly used for ASD animal models. This suggests that PPA may not only induce mitochondrial dysfunction, but also exert epigenetic histone deacetylase inhibitory functions, similar to valproic acid, which can alter gene expression (MacFabe et al., 2007).

Although it is expected that PPA exposure will induce changes in mitochondrial function and neurodevelopment, a lack of experiments have attempted to identify the changes in the expression of specific genes after PPA exposure to neuronal cells (MacFabe, 2013; Nankova et al., 2014). Therefore, in this study, we used a human neuroblastoma cell line, SH-SY5Y, and normal human neural progenitor (NHNP) cells to observe the changes in gene expression by using microarray experiments in conjunction with PPA treatment in an attempt to find the signaling pathways related to mitochondria dysfunction that affects neurodevelopment.

2. Material and methods

2.1. Cell culture

SH-SY5Y cells were obtained from the Korean cell line bank (<http://cellbank.snu.ac.kr>). The cells were cultured in Dulbecco's Modified Eagle's Medium (DMEM/F12, Lonza, USA) supplemented with 10% fetal bovine serum (Alphabio Regen, MA), 1% penicillin and streptomycin (Gibco, USA), 1 × non-essential amino acid (NEAA, Lonza, USA), and 1 mM sodium pyruvate (Sigma-Aldrich, USA). Normal Human Neural Progenitor (NHNP) cells were obtained in Lonza (Lonza, Walkersville, MD). Each primary cell was maintained in Neural Progenitor Maintenance Medium (NPMM, Lonza, USA) supplemented with 2% Neural Survival Factor-1 (NSF-1), 0.2% Gentamicin/Amphotericin-B (GA-1000), 25 ng/mL brain-derived neurotrophic factor (BDNF), and Primary Neuron Growth Medium Kit (PNGM™, Lonza, Walkersville, MD). All cells were incubated at a temperature of 37 °C with 5% CO₂.

2.2. Mitochondrial membrane potential assay

SH-SY5Y cells were plated at 5 × 10⁴ cells/well in a 96-well black plate and incubated for 24 h. The cells were treated with vehicle (DPBS) or 1, 5, and 10 mM PPA for 4 h. The mitochondrial membrane potential was measured using the JC-10 mitochondrial membrane potential assay kit (Abcam, MA). Fluorescence intensity was observed using a fluorescence microscope (Beckman coulter, USA) at 490/525 nm.

2.3. Transmission electron microscopy

For transmission electron microscopy samples, SH-SY5Y cells were seeded at 10⁶ cells/well in 6-well plates and incubated for 24 h. The cells were treated with vehicle (DPBS) or 1 and 5 mM PPA for 72 h and then fixed at 4 °C in 2.5% glutaraldehyde (Sigma, USA), followed by 2% osmium tetroxide for 2 h. The cells were dehydrated with a graded acetone series and embedded into Spurr medium (Electron Microscopy System). The samples were sectioned (60 nm) with an ultra-microtome (RMC MTXL, Arizona, USA), and double-stained with 2% uranyl acetate and lead citrate. The sections were viewed at 80 kV a transmission electron microscope Hitachi H-7600 (Hitachi, Tokyo, Japan). The number of mitochondria per 100 μm² was counted within a randomly selected grid square in every image of each group. In addition, the sizes of 80 randomly chosen mitochondria were measured in images obtained using the Image J program (National Institutes of Health). Mitochondria actual size was calculated using a calibration grid. Values were presented as the mean individual size of the mitochondria.

2.4. Total RNA and DNA isolation

SH-SY5Y cells (1 × 10⁶ cells/well) were seeded into 6-well plates and incubated for 24 h. NHNP cells were plated onto 24- and 6-well coated plates, and then stabilized for 10 days. To prepare the DNA, SH-SY5Y cells were treated with vehicle (DPBS) or 1, 5, and 10 mM PPA for 72 h. From the pelleted cells, total genomic DNA for DNA copy number analysis was isolated using DNeasy blood and tissue kit (Qiagen, Hilden, GER). To prepare the RNA, SH-SY5Y cells were treated with vehicle (DPBS) or 1 and 5 mM PPA for 4, 24, and 72 h. NHNP cells were treated for 4 h. Total cellular RNA for microarray analysis and qPCR was extracted using miRNeasy mini kit (Qiagen, USA). RNA samples were quantified, aliquoted, and stored at –80 °C until use. For quality control, RNA purity and integrity were evaluated by denaturing gel electrophoresis at OD 260/280 ratio and analyzed on Agilent 2100 Bioanalyzer (Agilent Technologies, Palo Alto, USA).

2.5. mRNA array

Total RNA was amplified and purified to yield biotinylated cRNA using the Ambion Illumina RNA amplification kit (Ambion, Austin, USA) according to the manufacturer's instructions. Briefly, Labeled cRNA samples (750 ng) from 550 ng of total RNA were hybridized to each humanHT-12 v.4 expression bead array according to the manufacturer's instructions (Illumina, Inc., San Diego, USA). Detection of array signal was carried out using Amersham fluorolink streptavidin-Cy3 (GE Healthcare Bio-Sciences, Little Chalfont, UK) following manual. Arrays were scanned according to the manufacturer's instructions.

2.6. miRNA array

The Affymetrix Genechip miRNA 4.0 array process was executed according to the manufacturer's protocol. RNA samples (1 μg) were used for labeling with the FlashTag™ Biotin RNA Labeling Kit (Genisphere, Hatfield, PA, USA). The labeled RNA was quantified, fractionated, and hybridized to the miRNA microarray according manufacturer protocol. The chips were stained using a Genechip Fluidics Station 450 (Affymetrix, Santa Clara, CA, USA) and scanned with an Affymetrix GCS 3000 scanner (Affymetrix, Santa Clara, CA, USA). Signal values were computed using the Affymetrix® GeneChip™ Command Console software.

2.7. Array data analysis

The overall chip performance qualities were monitored. Raw data were extracted using the software and protocol provided by the manufacturer [Illumina GenomeStudio (v20011.1) Gene Expression Module (v1.9.0)]. Statistical significance of the expression data was determined using local-pooled-error (LPE) test. For a differential expressed gene (DEG) set, hierarchical cluster analysis was performed using complete linkage and Euclidean distance as a measure of similarity. Gene-Enrichment and Functional Annotation analysis for significant probe list was performed using DAVID (<http://david.abcc.ncifcrf.gov/home.jsp>).

Raw data for miRNA array were automatically extracted as per the Affymetrix data extraction protocol using the software provided by Affymetrix GeneChip® Command Console® Software (AGCC). The CEL files import, miRNA level RMA + DABG-All analysis, and result export was done using Affymetrix® Expression Console™ Software. The comparative analysis between test sample and control sample was carried out using fold change and LPE test. False discovery rate (FDR) was done using Benjamini-Hochberg algorithm. Statistical tests and differentially expressed genes visualization were conducted using R statistical language v. 3.1.2.

In the integrated analysis, data of miRNA expression and mRNA

expression, in which normalization was completed using quality control advanced through filtering in independent analysis, was used. Probe list showing differential expression within the miRNA data set and mRNA data set were extracted (significant cut-off : $|\text{fold change}| \geq 2$, $\text{lpe } p\text{-value} < 0.05$). Putative microRNA - mRNA target pair was inferred in this data through the target information provided at miRDB (<http://mirdb.org/miRDB/>, v4.0). After this, negative correlation in pairs was checked and a final microRNA-mRNA regulatory association list was derived.

2.8. Quantitative real-time PCR (qPCR) for mtDNA and mRNA

cDNA was synthesized from isolated RNA using a RT² first strand kit (Qiagen, USA) according to manufacturer's protocol. To determine the relative expression of the target gene mRNA or mitochondrial DNA (mtDNA) to the control gene, qPCR was performed using the iQ[™] SYBR[®] Green Supermix (Bio-rad, USA) in a CFX96[™] Real-Time system (Bio-rad, USA), according to the following conditions: 95°C for 3 min, 40 cycles of 95°C for 15 s, annealing temperature for 1 min. The primer sequence that was used for amplification of each gene is described in the Supplementary Table. mRNA expression was normalized to GAPDH for the samples. Relative mRNA expression and mtDNA copy number were assessed by analysis using the $2^{-\Delta\Delta C_t}$ method.

2.9. Western blot analyses

To obtain samples for protein isolation, SH-SY5Y cells were seeded in a 100-mm dish at a density of 1×10^6 cells/mL for 24 h. PPA (1 and 5 mM) was added. For the negative control, SH-SY5Y cells were treated with vehicle (DPBS). After 24 h, the cells were harvested and homogenized using RIPA buffer (ATTO, Japan) with proteinase and phosphatase inhibitors (ATTO, Japan). The primary antibodies used were anti-Ab, COX4, LFNG, SIRT3, and β -actin (Cell Signaling, USA), ASCL1 (Abcam, Shanghai, CHN), and PGC1- α , and TFAM (Millipore, Billerica, USA). After quantification, proteins were resolved by SDS-PAGE and transfer to nitrocellulose membranes. After incubation secondary antibodies, it was visualized using the Pierce[™] ECL western blotting substrate (Thermo Scientific, USA). β -Actin was used as a loading control and the protein expression was calculated by ImageJ software from western blotting bands of the proteins of interest.

2.10. Statistical analysis

All data are presented as the mean \pm standard deviation (SD) of the results from a minimum of five independent experiments. Statistical analysis was performed using SPSS (version 20, Chicago, USA) for Windows. The statistical significance of differences between groups was evaluated by the analysis of two-tailed Student's *t*-test and Dunnett's test. A *p*-value less than 0.05 ($p < 0.05$) was considered statistically significant. Significant *p* values data are denoted in the graphs as follows: * $p < 0.05$, ** $p < 0.01$, and *** $p < 0.001$.

3. Results

3.1. PPA induced mitochondrial dysfunction in SH-SY5Y cells

The treatment doses of PPA were 1 mM and 5 mM, and the vehicle control was distilled water. It is observed dose dependent cytotoxicity by PPA treatment with statistical significances in SH-SY5Y cell (Supplementary Fig. 1). In order to know the effect of PPA exposure on mitochondrial function, we observed the changes in the mitochondrial membrane potential and electron microscopic mitochondrial appearances after PPA treatment in SH-SY5Y cells (Fig. 1A). It was observed that after 4 h of PPA exposure the mitochondrial membrane potential decreased in a dose-dependent manner (Fig. 1B). In the electron-microscopic analysis, the mean number of mitochondria in the EM image

was 121/100 μm^2 in the vehicle group, 98/100 μm^2 in the 1 mM PPA treatment group and 79/100 μm^2 in the 5 mM PPA treatment group. The mean mitochondrial sizes were $0.10 \pm 0.009 \mu\text{m}^2$ for the vehicle, $0.09 \pm 0.006 \mu\text{m}^2$ for 1 mM PPA treatment group, and $0.06 \pm 0.007 \mu\text{m}^2$ for 5 mM PPA treatment group. Thus, the mitochondria in the 5 mM PPA-treated cells were smaller than those in the control group and this difference was statistically significant (Fig. 1C). The mtDNA copy numbers in SH-SY5Y cells were seen to increase in a dose-dependent manner after 72 h of PPA exposure (Fig. 1D).

3.2. PPA induced changes in the gene expression of mitochondrial biogenesis in SH-SY5Y cells

The mRNA expression of key mitochondrial biogenesis-related proteins such as PGC-1 α , TFAM, and SIRT3 was measured in SH-SY5Y cells treated with PPA for 4 h. The mRNA of PGC-1 α and SIRT3 was significantly increased in the SH-SY5Y cells in response to PPA treatment for 4 h (Fig. 2A). In agreement with the mRNA data, protein expression of PGC-1 α and SIRT3 were significantly increased after treatment with 5 mM PPA for 24 h (Fig. 2B). Although the mRNA level of TFAM decreased after PPA treatment for 4 h, TFAM protein expression was increased. This suggests that PPA induced mitochondrial biogenesis-related gene expression such as PGC-1 α , TFAM, and SIRT3. With mtDNA copy number increasing, mitochondrial COX4 protein expression was also increased in the SH-SY5Y cells treated with 5 mM PPA for 24 h (Fig. 2B). However, it was not observed the change of SIRT1 expression in the PPA treated SH-SY5Y cells for 24 h (data not shown)

3.3. Gene expression profiling results by mRNA arrays

mRNA microarray was used to examine the effect of PPA on mRNA expression in SHSY5Y and NHNP cells. The SHSY5Y cells were treated with 1 mM and 5 mM of PPA for 4, 24, and 72 h. The NHNP cells were treated with 1 mM and 5 mM of PPA for 4 h. After normalization, a total of 2869 probes were selected by data processing. In the multi-dimensional scaling plot and hierarchical clustering analysis, it can be seen that the differences of gene expression pattern between SH-SY5Y and NHNP and the concentration dependent differential gene expression change patterns (Supplementary figure S2). For annotation of the set of functional gene in these experiments, we used the DAVID bioinformatics tool and observed most significant clusters (Enrichment Score (ES) > 7) of enriched Gene Ontology (GO) biological processes (BP) among the genes differentially abundant between PPA treatment and control within SH-SY5Y and NHNP (Supplementary figure S3-6). In this cluster, several GO terms associated with neurodevelopment (for example, GO:0,030,182'neuron differentiation, GO:0,006,928'cell motion, GO:0,031,175'neuron projection development) were selected with high statistically significance. Additional information in each cluster is provided in the Supplementary Table.

3.4. PPA induced a change in Notch signaling-related gene expression in SH-SY5Y cells

In the selection of genes to confirm for gene expression, a scheme was adopted, of three different time points after PPA treatment, with a maximum concentration (5 mM) treated group versus control. Only differentially expressed genes with more than 2 fold changed expression values were considered (Table 1). To further prove the reliability of the microarray data and ASCL1 and LFNG were selected. We evaluated the mRNA expression by real-time qPCR to confirm the expression changes of ASCL1 and LFNG. The mRNA of ASCL1 was significantly decreased while that of LFNG was significantly increased in the SH-SY5Y cells, in response to PPA treatment for 4 h (Fig. 3A). In the NHNP cells, it was confirmed that ASCL1 expression was significantly decreased and LFNG expression was significantly increased by 5 mM PPA exposure ($p < 0.05$). In agreement with the mRNA data, protein expression of ASCL1

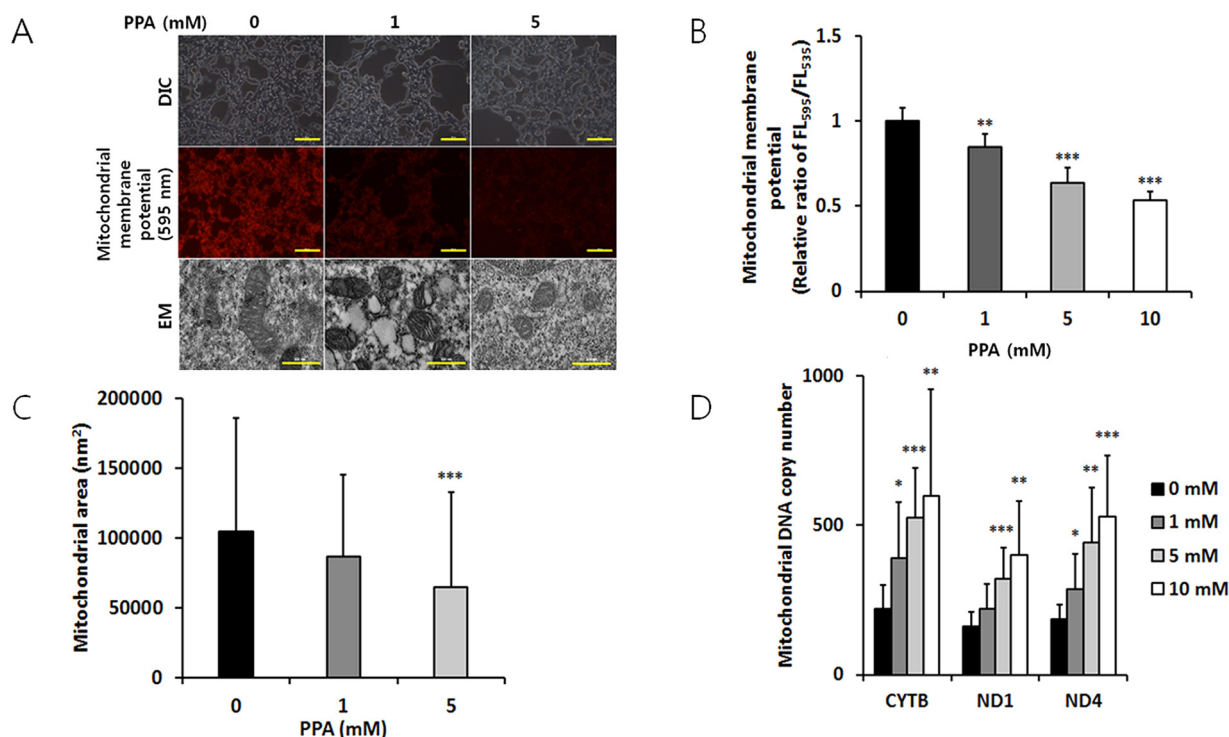


Fig. 1. PPA-mediated changes in SH-SY5Y cells. (A) Vehicle (DPBS) and PPA (1 and 5 mM) were treated to the cells. Cells treated for 4 h were stained with JC-10 dye to visualize the mitochondrial membrane potential. The mitochondrial morphology was confirmed using transmission electron microscopy (EM) in cells treated for 72 h. Scale bars = 100 μm (DIC, mitochondrial membrane potential); 500 nm (EM). (B) The mitochondrial membrane potential was assessed by JC-10 aggregate/monomer ratio (595/535 nm) in SH-SY5Y cells treated with PPA for 4 h. Data are presented mean ± SD (n = 9). (C) The size was measured in 80 randomly selected mitochondria in images obtained using electron microscopy in cells treated with PPA for 72 h. Data are presented as mean ± SD (n = 80). (D) The contents of Mitochondrial genes of three types (*CYTB*, *ND1*, and *ND4*) were measured by qPCR in cells cultured with PPA for 72 h, and the mitochondrial DNA copy number was evaluated. Data are presented as mean ± SD (n = 12). PPA-treated groups were statistically analyzed compared to the vehicle group (*p < 0.05, **p < 0.01, and ***p < 0.001).

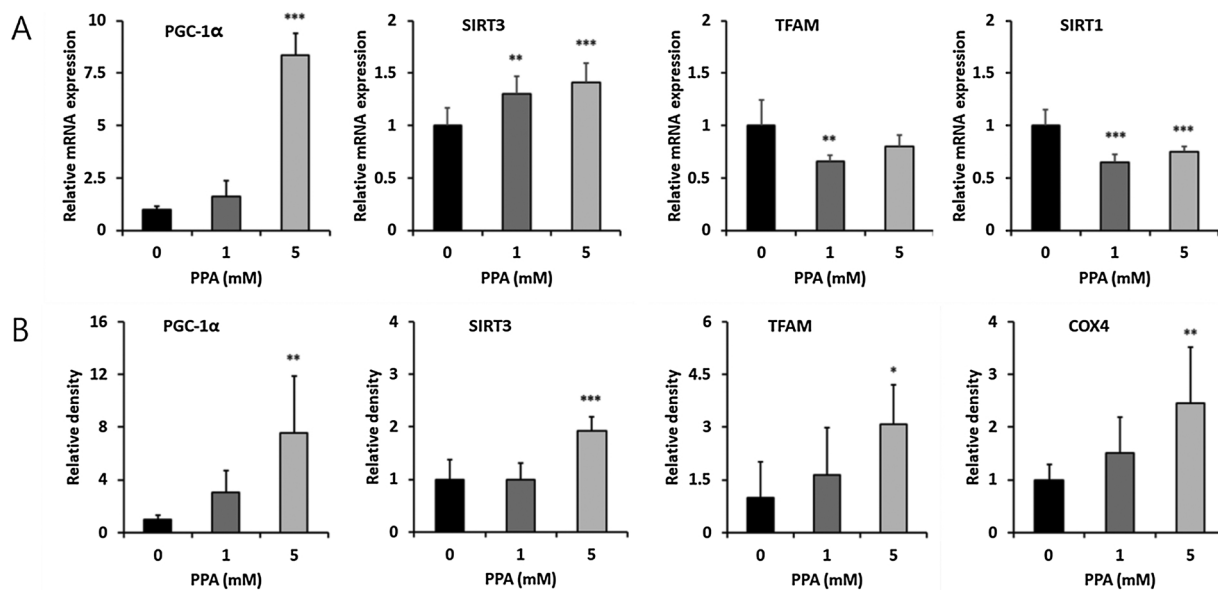


Fig. 2. Change in gene expression of PPA-treated SH-SY5Y cells. (A) The mRNA expression levels of the genes (*PGC-1α*, *SIRT3*, *TFAM*, and *SIRT1*) related to mitochondrial biogenesis (B) Western blotting was used to evaluate the level of protein expression related to mitochondrial biogenesis (*PGC-1α*, *SIRT3*, *TFAM*, and *COX4*) in the obtained proteins. β-Actin was used as the loading control to normalize the content of each sample. All data are presented mean ± SD (n = 6). Statistical significance is expressed in comparison with the vehicle group (*p < 0.05, **p < 0.01, and ***p < 0.001).

Table 1
Gene list for major changes of mRNA expression with PPA treatment by microarray.

Gene symbol	Value of fold change for 5 mM PPA treatment /control			
	NHNP		SHSY-5Y	
	4 h	4 h	24 h	72 h
ASCL1	-2.06	-4.77	-2.06	-6.16
EFS	-2.65	-4.27	-3.52	-3.56
FAIM	-2.04	-3.26	-2.28	-2.13
NFKB1	-2.05	-3.15	-3.03	-2.60
NAGPA	-2.65	-3.14	-3.03	-2.78
KCTD15	-2.09	-2.80	-2.11	-2.16
SPG3A	-2.75	-2.76	-2.22	-2.09
NSMAF	-2.13	-2.60	-2.39	-2.01
C6orf168	-2.00	-2.49	-2.33	-2.13
KLF11	-2.14	-2.14	-2.09	-2.98
GTF2IRD2B	-2.53	-2.13	-2.40	-2.46
H2AFY2	-2.05	-2.10	-3.21	-3.05
HIST1H2BD	2.08	2.08	2.02	3.27
BMF	2.43	2.63	2.58	2.46
S1PR3	2.12	3.75	2.44	2.11
TNFRSF19	2.43	3.79	3.73	3.27
CSRNP1	2.23	3.84	2.86	2.34
KIAA1683	2.07	4.03	2.48	3.63
LFNG	2.04	4.08	2.76	2.77

was significantly decreased after treatment with 5 mM PPA after 24 h, while LFNG expression increased in a dose-dependent manner (Fig. 3B).

3.5. Gene expression profiling results by miRNA arrays and integrative genomic analysis

The expression profiling of human-specific miRNAs was performed in PPA-treated SH-SY5Y cells using the Affymetrix GeneChip microarray assay. Similar to the mRNA array setting, SH-SY5Y cells and NHNP were harvested after PPA or vehicle treatment. The hierarchical clustering heatmap shows all differentially regulated miRNAs in the 12 independent samples (Supplementary figure S7). Further analysis showed that miRNAs were differentially expressed during PPA treatment compared with those in the control cells (Supplementary Table).

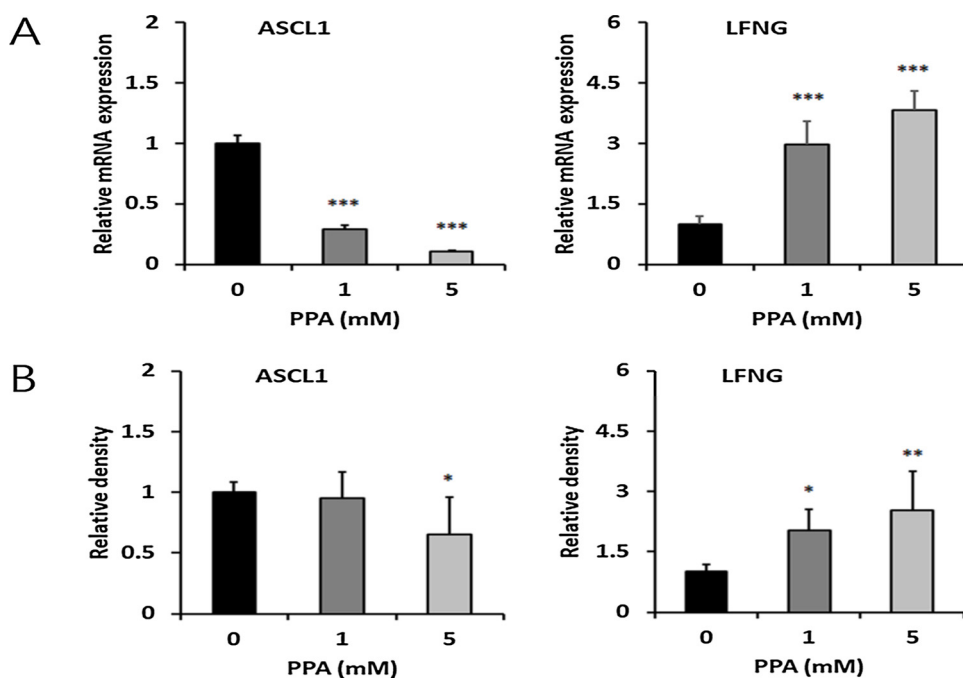


Fig. 3. Changes in gene expression related to PPA-induced Notch signaling in SH-SY5Y cells. (A) Relative mRNA expression of the genes (*ASCL1*, *LFNG*) involved in Notch signaling was measured in cells cultured with PPA for 4 h. (B) The proteins were isolated from whole cell lysates treated with PPA for 24 h, and the expression levels of proteins (*ASCL1*, *LFNG*) related to notch signaling were measured using western blot. β -Actin was used for the loading control to normalize the content of each sample. All data are presented as mean \pm SD (n = 6). PPA-treated groups were statistically analyzed in comparison with the vehicle group (* p < 0.05, ** p < 0.01, and *** p < 0.001).

In addition, the expression patterns of miRNA were different between NHNP and SH-SY5Y. According to the integration analysis with miRNA and mRNA data of NHNP, although the expression regulation of LFNG by miR-4472 can be suggested with moderate confidence from Ingenuity® Pathway Analysis (IPA®), there were no miRNA candidates for *ASCL1* expression regulation (Supplementary Table).

4. Discussion

In this study, we observed changes in gene expression related to Notch signaling (*ASCL1* and *LFNG*) and mitochondrial biogenesis (*SIRT3*, *PGC1- α* , *TFAM*, and *COX*) related to mitochondrial dysfunction in SH-SY5Y cells subjected to acute PPA exposure. Mitochondria play central roles not only through energetics and ATP production, but also through metabolites generated in the tricarboxylic acid cycle as well as via mitochondria-nuclear signaling related to mitochondria morphology, biogenesis, fission/fusion, and epigenetic regulation. Understanding mitochondria-cell signaling will provide insights into individual responses to environmental stressors (Shaughnessy et al., 2014). Mitochondrial dysfunction have been also implicated in ASD (Rossignol and Frye, 2012). A study performed on brains of autism patients postmortem revealed that several types of mitochondrial genes showed reduced expression in specific brain regions Mitochondrial dysfunction may be able to connect the diverse medical symptoms associated with ASD (Anitha et al., 2013, 2012; Frye and Rossignol, 2011). It is known that the elevated oxidative metabolism could be accompanied by an increase in reactive oxygen species (ROS) that are primarily generated by mitochondria.

It has been reported that mitochondria continually fuse and divide, and their quality, distribution, size, and motility are finely tuned (Fischer et al., 2012). Depending on the physiological conditions, mitochondrial fusion-fission equilibrium can be perturbed and mitochondrial dynamics can be changed (Suen et al., 2008). It is also suggested that PPA can have both beneficial and toxic effects on mitochondrial function, depending on the concentration, exposure duration, and microenvironment redox state (Frye et al., 2016). It is possible that oxidative stress induced by a high concentration of PPA causes dysfunction of mitochondrial components or the production of 3NP, an irreversible inhibitor of succinate dehydrogenase, although we could not assess 3NP generation in this in vitro cell culture system. In this

study, 5 mM PPA exposure induced cytotoxic effects and decreased ATP levels in SH-SY5Y cells (Supplementary Table S2), which was suggestive of mitochondrial dysfunction, and it is known that mitochondrial dysfunction induces changes in the number and size of mitochondria via mitochondrial dynamics. These mitochondrial dynamics may influence complex signaling pathways, affect gene expression, and define cell differentiation. Recent findings suggest that the crosstalk between mitochondria and nuclear signaling such as Notch signaling pathway is bidirectional (Basak et al., 2014; Kasahara and Scorrano, 2014).

In this study, it was observed that PPA induced mitochondrial dysfunction and increased gene expression related with mitochondrial biogenesis signaling, including PGC-1 α . TFAM, COX4 and SIRT3. SIRT3, a NAD⁺-dependent protein deacetylase and one of the mammalian sirtuins, is reported to be a downstream target gene of PGC-1 α and mediates the PGC-1 α effects in mitochondrial biogenesis (Austin and St-Pierre, 2012; Kong et al., 2010). It is known that forkhead transcription factor FOXO3, which transactivates antioxidant genes such as catalase and manganese superoxide dismutase, is a direct target of SIRT3 in the mitochondria. It also suggested that the SIRT3-mediated deacetylation of FOXO3 modulates mitochondrial quantity and quality through the nuclear translocation of FOXO3 (Rangarajan et al., 2015; Tseng et al., 2013). We also observed that exposure to PPA results in increased FOXO3 nuclear localization in SH-SY5Y cells (Supplementary Figure S8).

Renault et al. (2009) suggested that FOXO3 regulated the neuronal stem cell pool by the induction a program of genes that preserves quiescence, prevents premature differentiation, and controls oxygen metabolism (Renault et al., 2009). In addition, Webb et al. (2013) reported that FOXO3 shared common targets genes involved in the Notch pathway with the proneuronal bHLH transcription factor ASCL1 in genome-wide in primary cultures of adult neural progenitor cells (NPCs), and that FOXO3 inhibited ASCL1-dependent neurogenesis in NPCs and in vivo (Webb et al., 2013). The ASCL1 is one of core transcription factor that have been used to drive trans differentiation of mammalian fibroblasts directly into neurons. It has been suggested that ASCL1 is a crucial regulator of multiple aspects of neurogenesis in the central and peripheral nervous systems (Ali et al., 2014). It is also suggested that ASCL1 has the effect of enhancing neurite growth by damaged or surviving neurons as pro-neural factor (Tang, 2017). It has also been reported that Hes1 expression oscillates driving cyclic expression of the proneural gene Ascl1, and high Hes1 expression and resultant Ascl1 suppression promote quiescence in neural stem cells (Dhanesh et al., 2016; Sueda et al., 2019). Furthermore, in an unbiased genome-wide study combining chromatin immunoprecipitation with microarrays (ChIP–chip) for ASCL1 binding sites in in vivo study, it was observed that ASCL1 directly regulates genes associated with all of the major steps of neurogenesis such as Notch signaling which contributes to cell-cell communication in the residual neuronal stem cells during neurodevelopment (Castro et al., 2011; Juliandi et al., 2010).

Notch signaling is triggered when the ligands, e.g., Delta-like 1, expressed on the neighboring cell surface interact with Notch receptors. Upon ligand binding, Notch receptors undergo successive proteolytic cleavage and release the intracellular domain of Notch (NICD). The NICD translocates to the nucleus and activates the expression of Notch-mediated target genes such as the Hes family (Kageyama et al., 2007). Notch signaling is also essential for cell survival, stem cell maintenance, differentiation and development (Kopan and Ilagan, 2009). Notch signaling is also known to negatively regulate neurogenesis by promoting stem cell proliferation and gliogenesis (Pierfelice et al., 2011; Shimojo et al., 2011). It has been reported that LFNG, a key modifier of the Notch receptor, is selectively expressed in hippocampal neural stem cells (NSCs) and affects NSC recruitment, cell cycle duration, and terminal fate (Semerci et al., 2017). It has also been suggested that the expression of Lfng is regulated downstream of proneural genes by promotion of Notch activation in the neural progenitors. (Nikolaou et al., 2009). SIRT3-mediated nuclear translocated FOXO3 may induce

LFNG expression in this study because the LFNG gene is suggested as a target of FOXO3 transcription factor in the CHEA transcription factor targets database from Harmonizome database (Ma'ayan, 2016; Rouillard et al., 2016). In addition, other epigenetic change should be considered because it has been observed that miR 4472, which may be a candidate for LFNG expression negative regulation, was downregulated by PPA exposure in the miRNA array results in this study (Supplementary Tables 6 and 7). Epigenetic modification due to environmental effects is proposed as one of the important mechanisms of the pathogenesis of neurodevelopmental disorders such as ASD which may be affected by an interaction between genetic vulnerability and environmental factors for pathogenesis. In conclusion, it is suggested that acute PPA exposure may induce neurodevelopmental change by the bidirectional cross talk of mitochondria and Notch signaling pathway via FOXO3.

Funding

This work was supported by the National Research Foundation of Korea (NRF) grant funded by the Korea government, MSIP (NRF-2014R1A2A1A11053289), and MOE (No. 2017R1D1A3B03033533). JY Mun was supported by KBRI basic research program through Korea Brain Research Institute funded by Ministry of Science and ICT (19-BR-01-08).

Declaration of Competing Interest

The authors declare that they have no known competing financial interests or personal relationships that could have appeared to influence the work reported in this paper.

Acknowledgements

We thank Mi Sun Kang who helped with the experiments. Lastly, we are grateful to Macrogen company, which helped with the bioinformatics analysis, including IPA.

Appendix A. Supplementary data

Supplementary material related to this article can be found, in the online version, at doi:<https://doi.org/10.1016/j.neuro.2019.09.009>.

References

- Al-Ghamdi, M., Al-Ayadhi, L., El-Ansary, A., 2014. Selected biomarkers as predictive tools in testing efficacy of melatonin and coenzyme Q on propionic acid - induced neurotoxicity in rodent model of autism. *BMC Neurosci.* 15, 34. <https://doi.org/10.1186/1471-2202-15-34>.
- Al-Owain, M., Kaya, N., Al-Shamrani, H., Al-Bakheet, A., Qari, A., Al-Muaigil, S., Ghaziuddin, M., 2013. Autism spectrum disorder in a child with propionic acidemia. *JIMD Rep.* 7, 63–66. https://doi.org/10.1007/8904_2012_143.
- Aldbass, A.M., Bhat, R.S., El-Ansary, A., 2013. Protective and therapeutic potency of N-acetyl-cysteine on propionic acid-induced biochemical autistic features in rats. *J. Neuroinflamm.* 10, 42. <https://doi.org/10.1186/1742-2094-10-42>.
- Alfawaz, H.A., Bhat, R.S., Al-Ayadhi, L., El-Ansary, A.K., 2014. Protective and restorative potency of Vitamin D on persistent biochemical autistic features induced in propionic acid-intoxicated rat pups. *BMC Complement. Altern. Med.* 14, 416. <https://doi.org/10.1186/1472-6882-14-416>.
- Ali, F.R., Cheng, K., Kirwan, P., Metcalfe, S., Livesey, F.J., Barker, R.A., Philpott, A., 2014. The phosphorylation status of Ascl1 is a key determinant of neuronal differentiation and maturation in vivo and in vitro. *Development* 141, 2216–2224. <https://doi.org/10.1242/dev.106377>.
- Anitha, A., Nakamura, K., Thanseem, I., Matsuzaki, H., Miyachi, T., Tsujii, M., Iwata, Y., Suzuki, K., Sugiyama, T., Mori, N., 2013. Downregulation of the expression of mitochondrial electron transport complex genes in autism brains. *Brain Pathol.* 23, 294–302. <https://doi.org/10.1111/bpa.12002>.
- Anitha, A., Nakamura, K., Thanseem, I., Yamada, K., Iwayama, Y., Toyota, T., Matsuzaki, H., Miyachi, T., Yamada, S., Tsujii, M., Tsuchiya, K.J., Matsumoto, K., Iwata, Y., Suzuki, K., Ichikawa, H., Sugiyama, T., Yoshikawa, T., Mori, N., 2012. Brain region-specific altered expression and association of mitochondria-related genes in autism. *Mol. Autism* 3, 12. <https://doi.org/10.1186/2040-2392-3-12>.
- Austin, S., St-Pierre, J., 2012. PGC1 α and mitochondrial metabolism—emerging concepts

- and relevance in ageing and neurodegenerative disorders. *J. Cell. Sci.* 125, 4963–4971. <https://doi.org/10.1242/jcs.113662>.
- Basak, N.P., Roy, A., Banerjee, S., 2014. Alteration of mitochondrial proteome due to activation of Notch1 signaling pathway. *J. Biol. Chem.* 289, 7320–7334. <https://doi.org/10.1074/JBC.M113.519405>.
- Castro, D.S., Martynoga, B., Parras, C., Ramesh, V., Pacary, E., Johnston, C., Drechsel, D., Lebel-Potter, M., Garcia, L.G., Hunt, C., Dolle, D., Bithell, A., Ettwiller, L., Buckley, N., Guillemot, F., 2011. A novel function of the proneural factor Ascl1 in progenitor proliferation identified by genome-wide characterization of its targets. *Genes Dev.* 25, 930–945. <https://doi.org/10.1101/gad.627811>.
- Choi, J., Lee, S., Won, J., Jin, Y., Hong, Yunkyung, Hur, T.-Y., Kim, J.-H., Lee, S.-R., Hong, Yonggeun, 2018. Pathophysiological and neurobehavioral characteristics of a propionic acid-mediated autism-like rat model. *PLoS One* 13, e0192925. <https://doi.org/10.1371/journal.pone.0192925>.
- Dhanesh, S.B., Subashini, C., James, J., 2016. Hes1: the maestro in neurogenesis. *Cell. Mol. Life Sci.* 73, 4019–4042. <https://doi.org/10.1007/s0018-016-2277-z>.
- El-Ansary, A., Shaker, G., Siddiqi, N.J., Al-Ayadi, L.Y., 2013. Possible ameliorative effects of antioxidants on propionic acid / clindamycin - induced neurotoxicity in Syrian hamsters. *Gut Pathog.* 5, 32. <https://doi.org/10.1186/1757-4749-5-32>.
- El-Ansary, A.K., Ben Bacha, A., Koth, M., 2012. Etiology of autistic features: the persisting neurotoxic effects of propionic acid. *J. Neuroinflamm.* 9, 74. <https://doi.org/10.1186/1742-2094-9-74>.
- Fischer, F., Hamann, A., Osiewacz, H.D., 2012. Mitochondrial quality control: an integrated network of pathways. *Trends Biochem. Sci.* 37, 284–292. <https://doi.org/10.1016/j.tibs.2012.02.004>.
- Frye, R.E., Melnyk, S., MacFabe, D.F., 2013. Unique acyl-carnitine profiles are potential biomarkers for acquired mitochondrial disease in autism spectrum disorder. *Transl. Psychiatry* 3, e220. <https://doi.org/10.1038/tp.2012.143>.
- Frye, R.E., Rose, S., Chacko, J., Wynne, R., Benucci, S.C., Slattery, J.C., Tippett, M., Delhey, L., Melnyk, S., Kahler, S.G., MacFabe, D.F., 2016. Modulation of mitochondrial function by the microbiome metabolite propionic acid in autism and control cell lines. *Transl. Psychiatry* 6, e927. <https://doi.org/10.1038/tp.2016.189>.
- Frye, R.E., Rossignol, D.A., 2011. Mitochondrial dysfunction can connect the diverse medical symptoms associated with autism spectrum disorders. *Pediatr. Res.* 69, 41R–47R. <https://doi.org/10.1203/PDR.0b013e318212f16b>.
- Goldani, A.A.S., Downs, S.R., Widjaja, F., Lawton, B., Hendren, R.L., 2014. Biomarkers in autism. *Front. Psychiatry* 5, 100. <https://doi.org/10.3389/fpsy.2014.00100>.
- Juliandi, B., Abematsu, M., Nakashima, K., 2010. Epigenetic regulation in neural stem cell differentiation. *Dev. Growth Differ.* 52, 493–504. <https://doi.org/10.1111/j.1440-169X.2010.01175.x>.
- Kageyama, R., Ohtsuka, T., Kobayashi, T., Kageyama, R., 2007. The Hes gene family: repressors and oscillators that orchestrate embryogenesis. *Development* 134, 1243–1251. <https://doi.org/10.1242/dev.000786>.
- Kasahara, A., Scorrano, L., 2014. Mitochondria: from cell death executioners to regulators of cell differentiation. *Trends Cell Biol.* 24, 761–770. <https://doi.org/10.1016/j.tcb.2014.08.005>.
- Kong, X., Wang, R., Xue, Y., Liu, X., Zhang, H., Chen, Y., Fang, F., Chang, Y., 2010. Sirtuin 3, a new target of PGC-1 α , plays an important role in the suppression of ROS and mitochondrial biogenesis. *PLoS One* 5, e11707. <https://doi.org/10.1371/journal.pone.0011707>.
- Kopan, R., Ilagan, M.X.G., 2009. The canonical notch signaling pathway: unfolding the activation mechanism. *Cell* 137, 216–233. <https://doi.org/10.1016/J.CELL.2009.03.045>.
- Ma'ayan, A., 2016. Harmonizome. Ma'ayan Lab. Comput. Syst. Biol. [WWW Document] URL <https://amp.pharm.mssm.edu/Harmonizome/>.
- MacFabe, D.F., 2012. Short-chain fatty acid fermentation products of the gut microbiome: implications in autism spectrum disorders. *Microb. Ecol. Health Dis.* 23. <https://doi.org/10.3402/mehd.v23i0.19260>.
- MacFabe, D., 2013. Autism: metabolism, mitochondria, and the microbiome. *Glob. Adv. Health Med.* 2, 52–66. <https://doi.org/10.7453/gahmj.2013.089>.
- MacFabe, D.F., Cain, D.P., Rodriguez-Capote, K., Franklin, A.E., Hoffman, J.E., Boon, F., Taylor, R., Kavaliers, M., Ossenkopp, K.-P., 2007. Neurobiological effects of intraventricular propionic acid in rats: possible role of short chain fatty acids on the pathogenesis and characteristics of autism spectrum disorders. *Behav. Brain Res.* 176, 149–169. <https://doi.org/10.1016/j.bbr.2006.07.025>.
- Nankova, B.B., Agarwal, R., MacFabe, D.F., La Gamma, E.F., 2014. Enteric bacterial metabolites propionic and butyric acid modulate gene expression, including CREB-dependent catecholaminergic neurotransmission, in PC12 cells—possible relevance to autism spectrum disorders. *PLoS One* 9, e103740. <https://doi.org/10.1371/journal.pone.0103740>.
- Nikolaou, N., Watanabe-Asaka, T., Gerety, S., Distel, M., Koster, R.W., Wilkinson, D.G., 2009. Lunatic fringe promotes the lateral inhibition of neurogenesis. *Development* 136, 2523–2533. <https://doi.org/10.1242/dev.034736>.
- Pierfelice, T., Alberi, L., Gaiano, N., 2011. Notch in the vertebrate nervous system: an old dog with new tricks. *Neuron* 69, 840–855. <https://doi.org/10.1016/J.NEURON.2011.02.031>.
- Rangarajan, P., Karthikeyan, A., Lu, J., Ling, E.-A., Dheen, S.T., 2015. Sirtuin 3 regulates Foxo3a-mediated antioxidant pathway in microglia. *Neuroscience* 311, 398–414. <https://doi.org/10.1016/J.NEUCO.2015.10.048>.
- Renault, V.M., Rafalski, V.A., Morgan, A.A., Salih, D.A.M., Brett, J.O., Webb, A.E., Villeda, S.A., Thekkat, P.U., Guillerey, C., Denko, N.C., Palmer, T.D., Butte, A.J., Brunet, A., 2009. FoxO3 regulates neural stem cell homeostasis. *Cell Stem Cell* 5, 527–539. <https://doi.org/10.1016/J.STEM.2009.09.014>.
- Rossignol, D.A., Frye, R.E., 2012. Mitochondrial dysfunction in autism spectrum disorders: a systematic review and meta-analysis. *Mol. Psychiatry* 17, 290–314. <https://doi.org/10.1038/mp.2010.136>.
- Rouillard, A.D., Gundersen, G.W., Fernandez, N.F., Wang, Z., Monteiro, C.D., McDermott, M.G., Ma'ayan, A., 2016. The harmonizome: a collection of processed datasets gathered to serve and mine knowledge about genes and proteins. *Database*. <https://doi.org/10.1093/database/baw100>. 2016, baw100.
- Rouillet, F.I., Lai, J.K.Y., Foster, J.A., 2013. In utero exposure to valproic acid and autism — a current review of clinical and animal studies. *Neurotoxicol. Teratol.* 36, 47–56. <https://doi.org/10.1016/J.NTT.2013.01.004>.
- Semerci, F., Choi, W.T.-S., Bajic, A., Thakkar, A., Encinas, J.M., Depreux, F., Segil, N., Groves, A.K., Maletic-Savatic, M., 2017. Lunatic fringe-mediated Notch signaling regulates adult hippocampal neural stem cell maintenance. *Elife* 6, e24660. <https://doi.org/10.7554/eLife.24660>.
- Shaughnessy, D.T., McAllister, K., Worth, L., Haugen, A.C., Meyer, J.N., Domann, F.E., Van Houten, B., Mostoslavsky, R., Bultman, S.J., Baccarelli, A.A., Begley, T.J., Sobol, R.W., Hirschey, M.D., Ideker, T., Santos, J.H., Copeland, W.C., Tice, R.R., Balshaw, D.M., Tyson, F.L., 2014. Mitochondria, energetics, epigenetics, and cellular responses to stress. *Environ. Health Perspect.* 122, 1271–1278. <https://doi.org/10.1289/ehp.1408418>.
- Shimojo, H., Ohtsuka, T., Kageyama, R., 2011. Dynamic expression of notch signaling genes in neural Stem/Progenitor cells. *Front. Neurosci.* 5, 78. <https://doi.org/10.3389/fnins.2011.00078>.
- Shultz, S.R., MacFabe, D.F., Ossenkopp, K.-P., Scratch, S., Whelan, J., Taylor, R., Cain, D.P., 2008. Intracerebroventricular injection of propionic acid, an enteric bacterial metabolic end-product, impairs social behavior in the rat: implications for an animal model of autism. *Neuropharmacology* 54, 901–911. <https://doi.org/10.1016/j.neuropharm.2008.01.013>.
- Sueda, R., Imayoshi, I., Harima, Y., Kageyama, R., 2019. High Hes1 expression and resultant Ascl1 suppression regulate quiescent vs. Active neural stem cells in the adult mouse brain. *Genes Dev.* <https://doi.org/10.1101/gad.323196.118>.
- Suen, D.-F., Norris, K.L., Youle, R.J., 2008. Mitochondrial dynamics and apoptosis. *Genes Dev.* 22, 1577–1590. <https://doi.org/10.1101/gad.1658508>.
- Tang, B.L., 2017. The potential of targeting brain pathology with Ascl1/Mash1. *Cells* 6. <https://doi.org/10.3390/cells6030026>.
- Thomas, R.H., Meeking, M.M., Mephum, J.R., Tichenoff, L., Possmayer, F., Liu, S., MacFabe, D.F., 2012. The enteric bacterial metabolite propionic acid alters brain and plasma phospholipid molecular species: further development of a rodent model of autism spectrum disorders. *J. Neuroinflamm.* 9, 153. <https://doi.org/10.1186/1742-2094-9-153>.
- Tseng, A.H.H., Shieh, S.-S., Wang, D.L., 2013. SIRT3 deacetylates FOXO3 to protect mitochondria against oxidative damage. *Free Radic. Biol. Med.* 63, 222–234. <https://doi.org/10.1016/J.FREERADBIOMED.2013.05.002>.
- Webb, A.E., Pollina, E.A., Vierbuchen, T., Urbán, N., Ucar, D., Leeman, D.S., Martynoga, B., Sewak, M., Rando, T.A., Guillemot, F., Wernig, M., Brunet, A., 2013. FOXO3 shares common targets with ASCL1 genome-wide and inhibits ASCL1-Dependent neurogenesis. *Cell Rep.* 4, 477–491. <https://doi.org/10.1016/J.CELREP.2013.06.035>.
- Yoo, H.J., Park, M., Kim, S.A., 2017. Difference in mitochondrial DNA copy number in peripheral blood cells between probands with autism spectrum disorders and their unaffected siblings. *World J. Biol. Psychiatry* 18, 151–156. <https://doi.org/10.1080/15622975.2016.1234069>.